BBA Advances 7 (2025) 100159

Contents lists available at ScienceDirect

BBA Advances

journal homepage: www.sciencedirect.com/journal/bba-advances

Claudin-11, a hypomyelinating leukodystrophy 22 (HLD22)-responsible protein, uniquely interacts with shroom-2 to change cell phenotypes

Sakurako Kobayashi [a], Takanori Yokoi [a], Takeru Omata [a], Hideji Yako [a], Yuki Miyamoto [a,b], Junji Yamauchi [a,b,*]

[a] Laboratory of Molecular Neuroscience and Neurology, Tokyo University of Pharmacy and Life Sciences, Tokyo 192-0392, Japan
[b] Laboratory of Molecular Pharmacology, National Research Institute for Child Health and Development, Tokyo 157-8535, Japan

ARTICLE INFO

Keywords:
Claudin-11
Shroom-2
HLD22
Oligodendrocyte
Differentiation before myelination

ABSTRACT

Oligodendroglial cells are a type of glial cell in the central nervous system (CNS) that wrap neuronal axons with differentiated plasma membranes known as myelin sheaths. While the physiological functions of oligodendrocytes, such as generating saltatory conduction and protecting neuronal axons, are well understood, the physiological and/or pathophysiological molecular mechanisms governing their differentiation before myelination remain unclear. In this study, we describe for the first time that claudin-11, a protein associated with hypomyelinating leukodystrophy 22 (HLD22), interacts with shroom-2, a presumable adaptor protein containing the PSD95, DLG1, and ZO-1 (PDZ) domain. Knockdown of claudin-11 using specific siRNA resulted in a decrease in morphological changes and marker proteins in the FBD-102b oligodendroglial model undergoing differentiation. Transfection of the C-terminal PDZ ligand sequence of claudin-11, which was found to interact with the PDZ domain of shroom-2, also reduced these phenotypic changes. The HLD22-associated mutated sequence in claudin-11 failed to interact with the PDZ domain of shroom-2. Furthermore, knockdown of shroom-2 or transfection of the PDZ domain of shroom-2, which is involved in the interaction with claudin-11, resulted in decreased morphological changes and marker protein expression. These changes were linked to the phosphorylation states of Akt kinase, a key signaling molecule in oligodendroglial cell differentiation and myelination. These results suggest that the interaction between claudin-11 and shroom-2 plays a key role in shaping cell morphology, providing insights into the molecular mechanisms underlying oligodendroglial differentiation before myelination, as well as potential pathological mechanisms associated with HLD22 at the molecular and cellular levels.

1. Introduction

During the development of the central nervous system (CNS), neuronal and glial cells work together, undergoing continuous morphological changes to form mature neural tissue [1,2]. Oligodendroglial cells (also called oligodendrocytes) are a type of CNS glial cell that not only provide various nutrients to neuronal cells but also wrap neuronal axons with fully differentiated plasma membranes, known as myelin sheaths [3,4]. These myelin sheaths are essential for saltatory conduction, enabling rapid signal transmission [1–6]. However, failure in myelination can lead to severe diseases, including inflammatory demyelinating conditions like multiple sclerosis [7,8] and genetic hypomyelinating and/or demyelinating diseases [9–14].

Genetic hypomyelinating diseases are now referred to as hypomyelinating leukodystrophies (HLDs) [9–12]. The prototypic HLD is Pelizaeus-Merzbacher disease (PMD), also known as HLD1 [9,10]. HLD1 is associated with mutations in the *proteolipid protein 1 (plp1)* gene, which encodes a four-spanning membrane protein within sheaths. HLD2 results from mutations in the gap junction protein gamma 2 (GJC2, also known as connexin 47), a four-spanning membrane protein, although GJC2 is not considered a myelin structural protein like PLP1 [13,14]. HLD22 is caused by mutations in the *claudin-11* gene [15], which is predicted to encode a four-spanning membrane protein in the myelin sheaths [16–18]. To date, three cases of HLD22 have been reported [15]. In brain imaging, patients with HLD22 typically exhibit hypomyelination at 3 to 4 years of age, followed by delayed myelination [15]. They

* Corresponding author at: Laboratory of Molecular Neuroscience and Neurology, Tokyo University of Pharmacy and Life Sciences, 1432-1 Horinouchi, Hachioji, Tokyo 192-0392, Japan,
E-mail address: yamauchi@toyaku.ac.jp (J. Yamauchi).

https://doi.org/10.1016/j.bbadva.2025.100159
Received 24 December 2024; Received in revised form 11 March 2025; Accepted 24 March 2025
Available online 24 March 2025

Table 1
Key materials used in this study.

Reagents or materials	Companies or sources	Cat. Nos.	Lot. Nos.	Concentrations used
Key antibody				
Anti-PLP1	Atlas Antibodies	HPA004128	B115828	Immunoblotting (IB), 1:500
Anti-MBP	BioLegends	836,504	B225469	IB, 1:500
Anti-CNPase	Santa Cruz Biotechnology	sc-166,019	2216	IB, 1:1000
Anti-GSTpi	MBL	312	067	IB, 1:500
Anti-actin (also called pan-beta type actin)	MBL	M177–3	007	IB, 1:5000
Anti-GAPDH	Santa Cruz Biotechnology	sc-32,233	2523	IB, 1:10,000
Anti-phospho-pan Akt (Akt1 sequence around pSer473 as the antigen)	Cell Signaling technology	4060T	27	IB, 1:500
Anti-pan Akt	Cell Signaling technology	4691T	28	IB, 1:500
Anti-FLAG tag (also called DDDDK tag)	MBL		002	IB, 1:10,000
Anti-GFP tag	MBL	M048–3	003	IB, 1:1000
Anti-GFP tag	Nakalai Tesque	04,404–26	M4K3355	Immunoprecipitation (IP), 1 microgram per 400 microgram of total crude proteins
Anti-Hexahis tag (also called His tag)	MBL	D291–3	002	IP, 1 microgram per 400 microgram of total crude proteins
Anti-Rabbit IgG (Goat) HRP-conjugated and pre-absorbed	Nakalai Tesque	21,860–24	M3H6046	IB, 1:10,000
Anti-Mouse IgG (Goat) HRP-conjugated and pre-absorbed	Nakalai Tesque	21,860–61	L4B5968	IB, 1:10,000
Peptide				
NH2-MHHHHHHPTHAKSAHV-COOH (purity, 92.5 %)	Genscript	J470U381G0_1	PE2053	Final concentration, 1 mM
Plasmid				
pcDNA3.1(+)-N-DYK-human Shroom2 PDZ domain (1–100 amino acids)	Genscript	J377 × 912G0–6	R633123	1.25 μg of DNA per 6 cm dish
pcDNA3.1(+)-human Cldn11	Genetated in this study			1.25 μg of DNA per 6 cm dish
pcDNA3.1(+)-N-eGFP-human Cldn11 (last 30 mino acids)	Genscript	J377 × 912G0–2	RG396971	1.25 μg of DNA per 6 cm dish
pcDNA3.1(+)-N-eGFP-human Cldn11 (last 30 mino acids) 208GlnExt39	Genscript	J377 × 912G0–4	RG396977	1.25 μg of DNA per 6 cm dish

present with intellectual disabilities, limb spasticity, and global developmental delays. Nystagmus was observed in two patients, and fine nystagmus in one. Characteristically, hyperopia and astigmatism are common features in all three reported HLD22 patients [9,10,15].

Despite the known symptoms including hypomyelination (thin myelin sheath formation) and delayed myelination, it remains unclear whether claudin-11 is actively involved in regulating oligodendroglial cell differentiation prior to hypomyelination and delayed myelination phenotypes at molecular and cellular levels. Thus, it remains unclear whether and how the loss-of-function of the claudin-11 protein is actually related to the differentiation of oligodendroglial cells before the onset of myelination [15]. HLD22 is specifically caused by one of two different nucleotide mutations within the stop codon, which result in the generation of a claudin-11 protein with 39 additional amino acids at the carboxyl terminal [15]. As a result, it is predicted that the ability of the carboxyl terminus of claudin-11 to bind to the PSD95, DLG1, and ZO-1 (PDZ) domains may be lost. Herein, we describe for the first time that knockdown of claudin-11 reduces morphological changes in the FBD-102b cell line, a model undergoing oligodendroglial differentiation and forming widespread myelin-like plasma membranes [19–22]. Of note, the carboxyl terminus of the wild type claudin-11 protein, but not that of the HLD22-associated claudin-11 mutated protein, interacted with the PDZ domain of presumable scaffold and/or adaptor protein shroom-2 [23,24]. We further investigated the interaction between claudin-11 and shroom-2, as well as the role of knockdown of shroom-2 itself, in influencing morphological differentiation.

2. Materials and methods

2.1. Key materials

The key materials including antibodies and plasmids are listed in Table 1.

2.2. Cell line culture and induction of differentiation

Mouse oligodendroglial FBD-102b cells (kindly provided by Dr. Yasuhiro Tomooka [Riken, Saitama, Japan]) were cultured on 6-cm- or 10-cm-diameter cell culture dishes (the Nunc brand of Thermo Fisher Scientific, Waltham, MA, USA) in high-glucose Dulbecco's modified Eagle's and F-12 mixed medium (DMEM/F12; Nacalai Tesque, Kyoto, Japan or Fujifilm, Tokyo, Japan) supplemented with 10 % heat-inactivated FBS (Thermo Fisher Scientific) and penicillin-streptomycin solution (Nacalai Tesque) in a 5 % CO_2 atmosphere at 37 °C.

To induce differentiation, FBD-102b cells were cultured in DMEM/F12 with 1 % FBS and penicillin-streptomycin solution in a 5% CO_2 atmosphere at 37 °C for several days, unless otherwise specified. Under these conditions, the percentage of cells incorporating trypan blue was estimated to be <5 % in each experiment. Cell morphologies were visualized using a microscope system equipped with an i-NTER lens (Micronet, Saitama, Japan) and i-NTER SHOT 2 software (ver. 12, Micronet). In each image (850 $^{\mu m}$ x 1500 $^{\mu m}$ [an i-NTER field]) captured with the microscope, cells with membrane structures capable of enclosing circles with diameters of 25 $^{\mu m}$ or more were considered differentiated using Image J software (ver. Java 8; downloaded from the NIH image website, https://imagej.nih.gov/) [23,24]. One field from each of the 10 culture samples was blindly selected, and the percentages of differentiated cells were statistically plotted. The images shown in the figures are representative of multiple captured images.

2.3. Reverse transcription and polymerase chain reaction (RT-PCR)

Total cellular RNA was prepared from cells grown on a 10-cm-diameter culture dish using Isogen (Nippon Gene, Tokyo, Japan) according to the manufacturer's instructions. Single strand cDNAs were generated from their RNAs (1 microgram of RNAs per one reaction) using the PrimeScript RT Master Mix kit (Takara Bio, Kyoto, Japan) in accordance

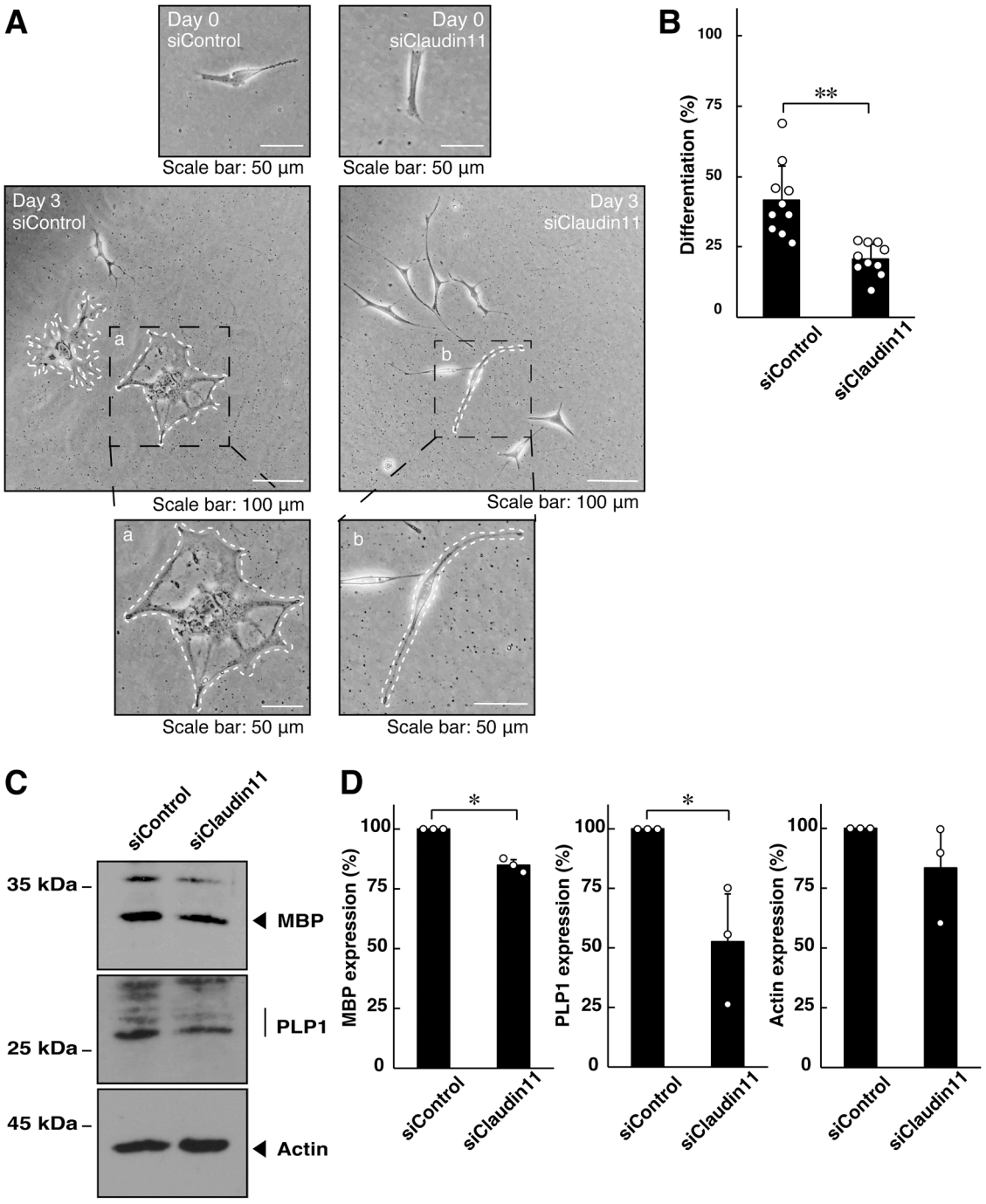

Fig. 1. Knockdown of claudin-11 decreases cell morphology and marker protein expression. (A, B) FBD-102b cells were transfected with control luciferase siRNA (siControl) or claudin-11 siRNA (siClaudin11) and cultured for 0 or 3 days following the induction of differentiation. Cells meeting differentiation criteria were counted and statistically depicted in the graph (** $p < 0.01$; $n = 10$ fields). Panels a and b (lower photographs) are enlarged images of squares a and b surrounded by black dotted lines (middle photographs). Some cells are surrounded by white dotted lines. (C and D) And, cell lysates following the induction of differentiation were immunoblotted with the respective antibodies against differentiation marker proteins MBP and PLP1, as well as the internal control actin. The immunoreactive bands of interest were quantified and graphed, with other immunoreactive bands set to 100 % (* $p < 0.05$; $n = 3$ blots).

with the manufacturer's instructions. PCR amplification was performed using 1:40 of the RT product with Gflex DNA polymerase (Takara Bio) for 35 cycles. Each cycle consisted of a denaturation step at 98 °C (0.2 min), an annealing step at 56 to 65 °C (0.25 min), depending on the annealing temperature, and an extension step at 68 °C (0.5 min). The resulting PCR products were loaded onto premade agarose gels (Nacalai Tesque).

2.4. Plasmid and small interfering (si)RNA transfection

Cells were transfected with plasmids using the ScreenFect A (for plasmid transfection) or ScreenFect A siRNA (for siRNA transfection) transfection kit (Fujifilm) in accordance with the manufacturer's instructions. The medium was replaced 4 h after transfection and was generally used for 48 h or more for cell biological and biochemical experiments, unless otherwise specified. Using plasmids encoding GFP (Takara Bio) and control siRNAs conjugated with HiLyte Fluor 488

(Nippon Gene, Tokyo, Japan), transfection efficiencies in FBD-102b cells were 85.2 % ± 2.15 % and 96.5 % ± 3.62 %, respectively [25]. In some experiments, multiple sets of transfected cells were microscopically observed using the i-NTER system (Micronet, Inc., Tokyo, Japan) and analyzed with i-NTER SHOT 2 software (ver. 2024, Micronet, Inc.). Under these conditions, the estimated percentage of attached cells incorporating trypan blue was <5 % in each experiment.

2.5. Cell lysis and immunoprecipitation

Cells were lysed in buffer (50 mM HEPES-NaOH pH 7.5, 150 mM NaCl, 5 mM $MgCl_2$, and 1 mM dithiothreitol) containing protease inhibitors (1 mM phenylmethanesulfonylfluoride, 2 mM leupeptin, and 1 mM EDTA), protein phosphatase inhibitors (1 mM Na_3VO_4 and 10 mM NaF), and mild detergents (0.1 % NP-40 and 1 % CHAPS) [22]. For immunoprecipitation, centrifuged collected cell supernatants (200 microgram per sample) were mixed and gently rotated with protein G resin (GE Healthcare, Chicago, IL, USA) conjugated to the respective antibodies for 1 hour at 4 °C. The complexes containing protein G resin were washed with lysis buffer and were denatured in sample buffers (Fujifilm).

2.6. Polyacrylamide electrophoresis and immunoblotting

The samples (20 microgram per sample) from the supernatants or immnoprecipitated samples were separated on pre-made sodium dodecylsulfate Tis polyacrylamide gels (Nacalai Tesque). The electrophoretically separated proteins were transferred to a polyvinylidene fluoride membrane (Fujifilm), blocked with Blocking One (Nacalai Tesque), and immunoblotted using primary antibodies, followed by peroxidase enzyme–conjugated secondary antibodies. Peroxidase-reactive bands, which were detected using Chemilumi One (Nacalai Tesque) or TMB Easy kit (Nacalai Tesque), were captured using a CanoScan system (Canon, Tokyo, Japan) and scanned with CanoScan software (ver. 2023; downloaded from the Canon website). The blots shown in the figures are representative of multiple blots. We performed multiple sets of experiments in immunoblotting studies, and immunoreactive bands were quantified using Image J software.

2.7. Purification of recombinant protein

Recombinant FLAG-tagged shroom-2 PDZ domain (1st-110th amino acid) were expressed in 293 cell-derived G3Thi cells (Takara Bio) [21]. The cell precipitates harvested by centrifugation were extracted with extraction buffer A (50 mM tris-HCl pH 7.5, 5 mM $MgCl_2$, 0.1 mM dithiothreitol, 1 mM phenylmethylsulfonylfluoride, 2 mM leupeptin, 1 mM EDTA, and 0.5 % NP-40). Unless otherwise indicated, all biochemical experimental steps were performed at 4 °C. Supernatants cleared by centrifugation were mixed with a DDDDK tagged protein purification kit (MBL, Tokyo, Japan). The bound proteins were washed with extraction buffer A and eluted with extraction buffer A containing elution solution in the purification kit. The buffer contained in the elution fractions was exchanged with reaction buffer A (50 mM tris-HCl pH 7.5, 3 mM $MgCl_2$, 0.1 mM $MnCl_2$, 150 mM NaCl, 0.1 mM DTT, 1 mM PMSF, and 1 mM EDTA) by dialysis. They were stored at −80 °C until use.

2.8. 3D complex structure prediction

The amino acid sequences of human shroom-2 (Acc. No. Q13796) and Claudin-11 (Acc. No. O75508) were obtained from the UniProt website (https://www.uniprot.org/). Using available Colab Fold ver. 1.5.5 based on AlphaFold2 (https://alphafold.ebi.ac.uk/), the complex structures of the minimum PDZ domain (RLVEVQLSGGAPWGFTLKG-GREHGEPLVITKIEEGSKAAAVDKLLAGDEIVGINDIGLSGFR-QEAICLVKGSHKTLKLVVK) of shroom-2 and the last 8 amino acids (THAKSAHV) of claudin-11 were simulated. The PyMOL molecular graphics system ver. 3.0 (Schrödinger, Inc., Broadway, NY, USA) was used to create the cartoon models.

2.9. Statistical analyses

Values are presented as means ± standard deviation (SD) from independent experiments. Intergroup comparisons were conducted using the unpaired Student's or Welch's *t*-test in Excel (ver. 2024, Microsoft, Redmond, WA, USA). For multiple comparisons, a one-way analysis of variance (ANOVA) was performed, followed by Fisher's comparison test using StatPlus plug-in software (ver. 2021, Alexandria, VA, USA). Differences were considered statistically significant at $p < 0.05$.

2. 10. Ethics statement

Techniques using genetically modified techniques were performed in accordance with a protocol approved by the Tokyo University of Pharmacy and Life Sciences Gene and Animal Care Committee (Approval Nos. LS28–20 and LSR3–011).

3. Results

3.1. Knockdown of claudin-11 decreases morphological changes with decreased oligodendroglial differentiation marker proteins

We investigated the role of claudin-11 [23,24] in morphological differentiation in oligodendroglial cells. Mouse FBD-102b cells were transfected with siRNA specific to claudin-11, with the PDZ ligand at the carboxyl terminal position, or with a control siRNA, and allowed to differentiate for 0 or 3 days. Knockdown of claudin-11 (Figure S1) resulted in decreased morphological changes (Fig. 1, A and B; Figure S2). Knockdown of claudin-11 also reduced the expression levels of oligodendroglial differentiation marker proteins, myelin basic protein (MBP), and myelin proteolipid protein 1 (PLP1), while the levels of the internal control actin protein remained comparable (Fig. 1, C and D), indicating the key role of claudin-11 in oligodendroglial cell differentiation.

In cells knocked down with siRNA specific to claudin-11, re-introduction of the plasmid encoding full-length human claudin-11 led to morphological changes. In contrast, transfection of the plasmid encoding only the carboxy terminal region of claudin-11 failed to recover the cellular phenotypes knocked down with claudin-11 siRNA (Figure S3), suggesting that differentiation requires both claudin-11 itself and a molecule that interacts with the claudin-11 PDZ ligand sequence.

We further examined the effect of claudin-11 knockdown on the expression levels of other differentiation marker proteins using three sets of cell lysates. Immunoblotting experiments for each antibody were performed using the same cell lysates. Knockdown of claudin-11 resulted in decreased expression levels of 2′, 3′-cyclic nucleotide 3′-phosphodiesterase (CNPase) and glutathione S-transferase pi (GSTpi), while the levels of the control protein glyceraldehyde-3-phosphate dehydrogenase (GAPDH) remained comparable (Figure S4, A and B), as supported by immunoblotting data using antibodies against MBP or PLP1.

3.2. Claudin-11 interacts with shroom-2 to mediate morphological changes

Since claudin family proteins contain a PDZ ligand at their carboxy terminus, we searched for proteins with a PDZ domain in the gene data present in differentiating oligodendroglial cells (Ref. 21, GEO Acc. No. GSE114957). We identified the possible scaffold and/or adaptor protein shroom-2, which contains a PDZ domain [23,24], as a gene highly upregulated following differentiation induction in oligodendroglial precursor cells. Shroom-2 has a typical PDZ domain in its protein structure. We then isolated this PDZ domain and performed an

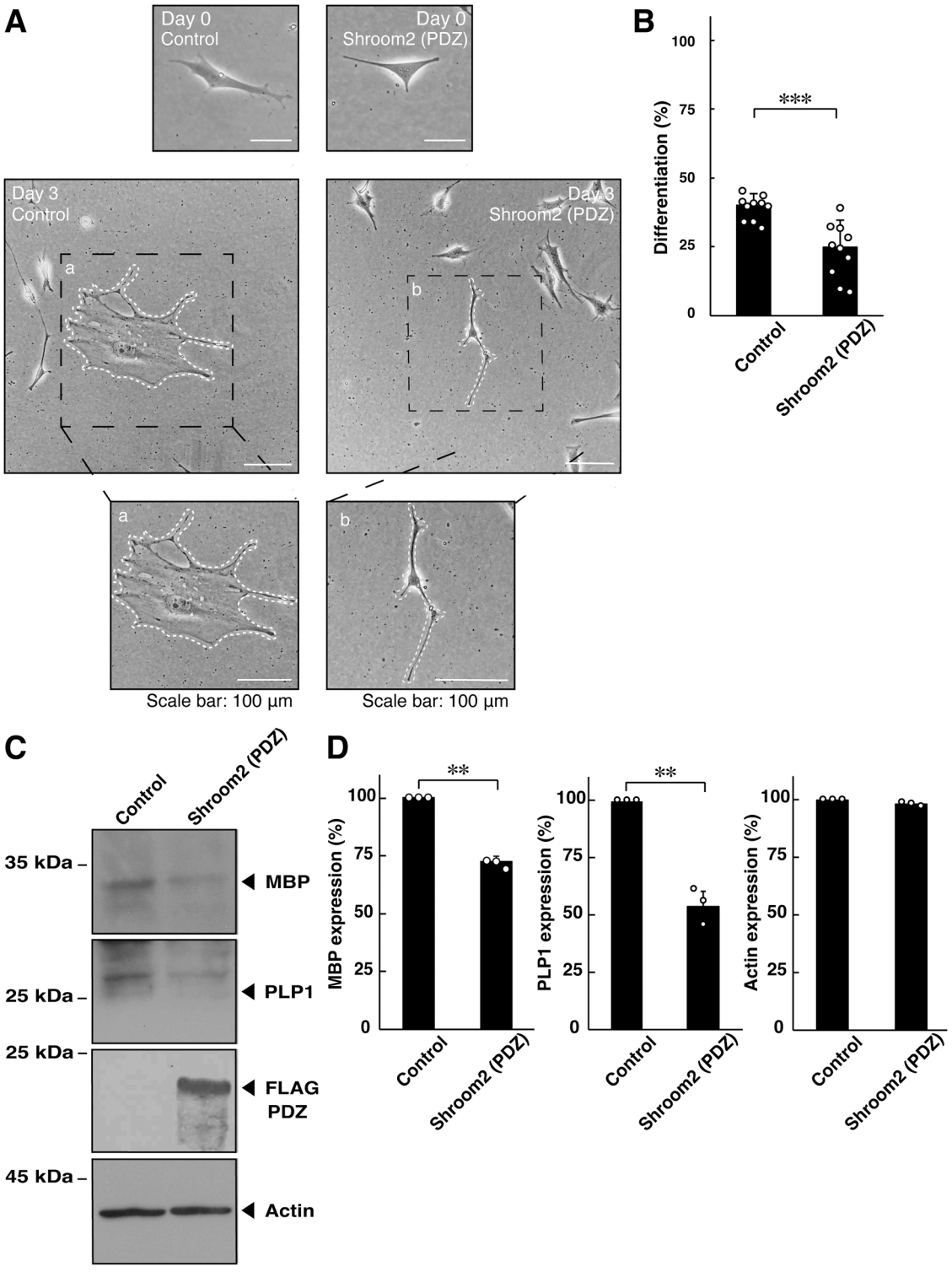

Fig. 2. Transfection of the PDZ domain of shroom-2 decreases cell morphology and marker protein expression. (A, B) Cells were transfected with a control vector (Control) or the plasmid encoding the FLAG-tagged PDZ domain of shroom-2 (shroom-2 [PDZ]) and cultured for 0 or 3 days following the induction of differentiation. Cells meeting differentiation criteria were counted and statistically depicted in the graph (*** $p < 0.001$; $n = 10$ fields). Panels a and b (lower photographs) are enlarged images of squares a and b surrounded by black dotted lines (middle photographs). Some cells are surrounded by white dotted lines. (C and D) And, cell lysates following the induction of differentiation were immunoblotted with the respective antibodies against differentiation marker proteins, tagged protein (FLAG-PDZ), and actin. The immunoreactive bands of interest were quantified and graphed, with other immunoreactive bands set to 100 % (** $p < 0.01$; $n = 3$ blots).

immunoprecipitation with the carboxy terminal region of claudin-11 (Figure S5). FLAG-tagged PDZ domain formed an immune-complex with GFP-tagged wild type PDZ ligand but not with HLD22 type. The result is consistent with a predicted complex structure of minimum PDZ domain of shroom-2 and wild type PDZ ligand of claudin-11. We then tried to measure the binding value of the minimum PDZ domain (recombinant protein) of shroom-2 and the minimum carboxy terminal 8 amino acids (immobilized peptide) of claudin-11 using

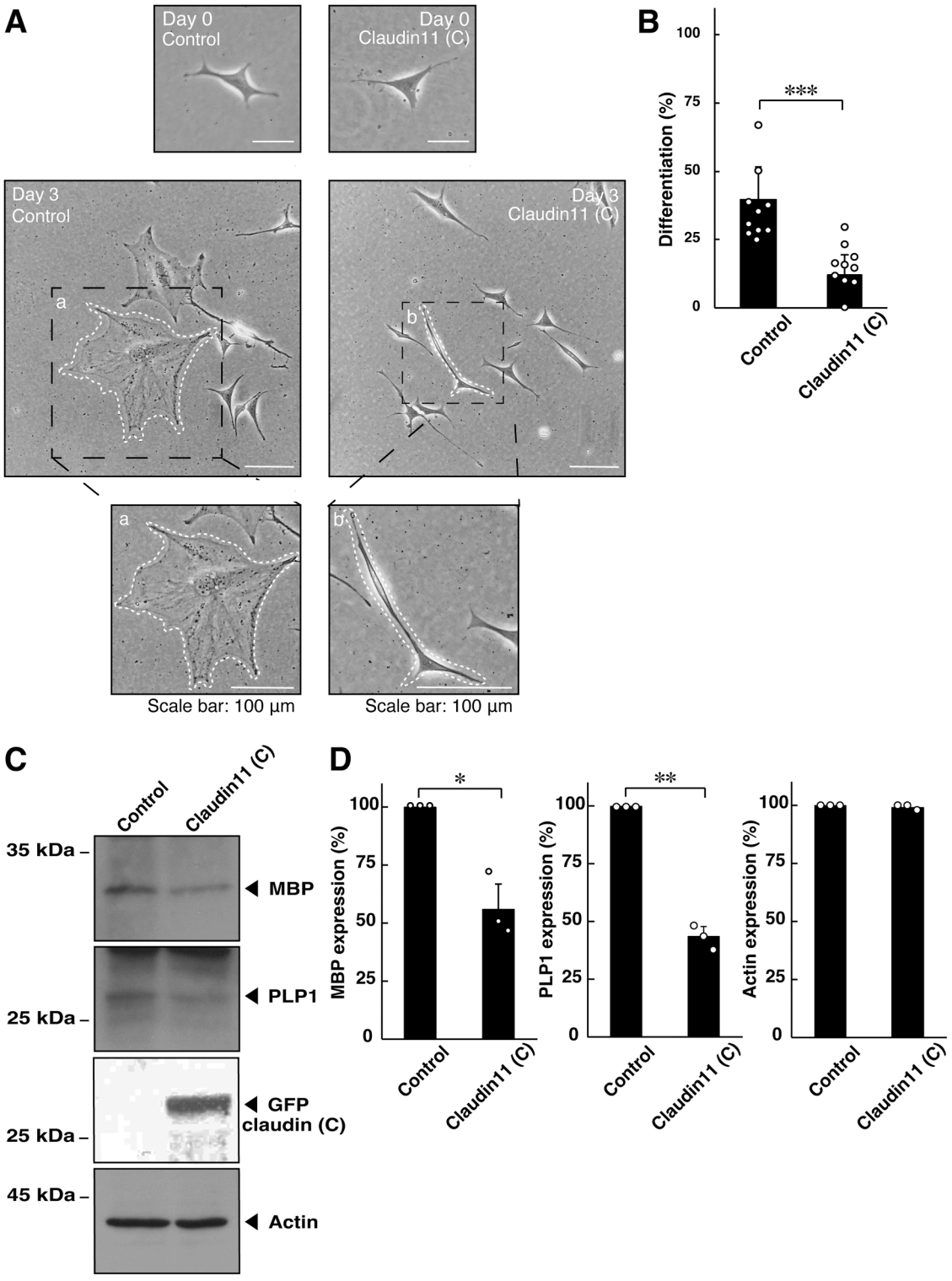

Fig. 3. Transfection of the PDZ ligand sequence of claudin-11 decreases cell morphology and marker protein expression. (A, B) Cells were transfected with a control vector (Control) or the plasmid encoding the GFP-tagged PDZ ligand sequence of claudin-11 (claudin-11 [C]) and cultured for 0 or 3 days following the induction of differentiation. Cells meeting differentiation criteria were counted and statistically depicted in the graph (*** $p < 0.001$; $n = 10$ fields). Panels a and b (lower photographs) are enlarged images of squares a and b surrounded by black dotted lines (middle photographs). Some cells are surrounded by white dotted lines. (C and D) And, cell lysates following the induction of differentiation were immunoblotted with the respective antibodies against differentiation marker proteins, tagged protein (GFP-claudin [C]), and actin. The immunoreactive bands of interest were quantified and graphed, with other immunoreactive bands set to 100 % (** $p < 0.01$, * $p < 0.05$; $n = 3$ blots).

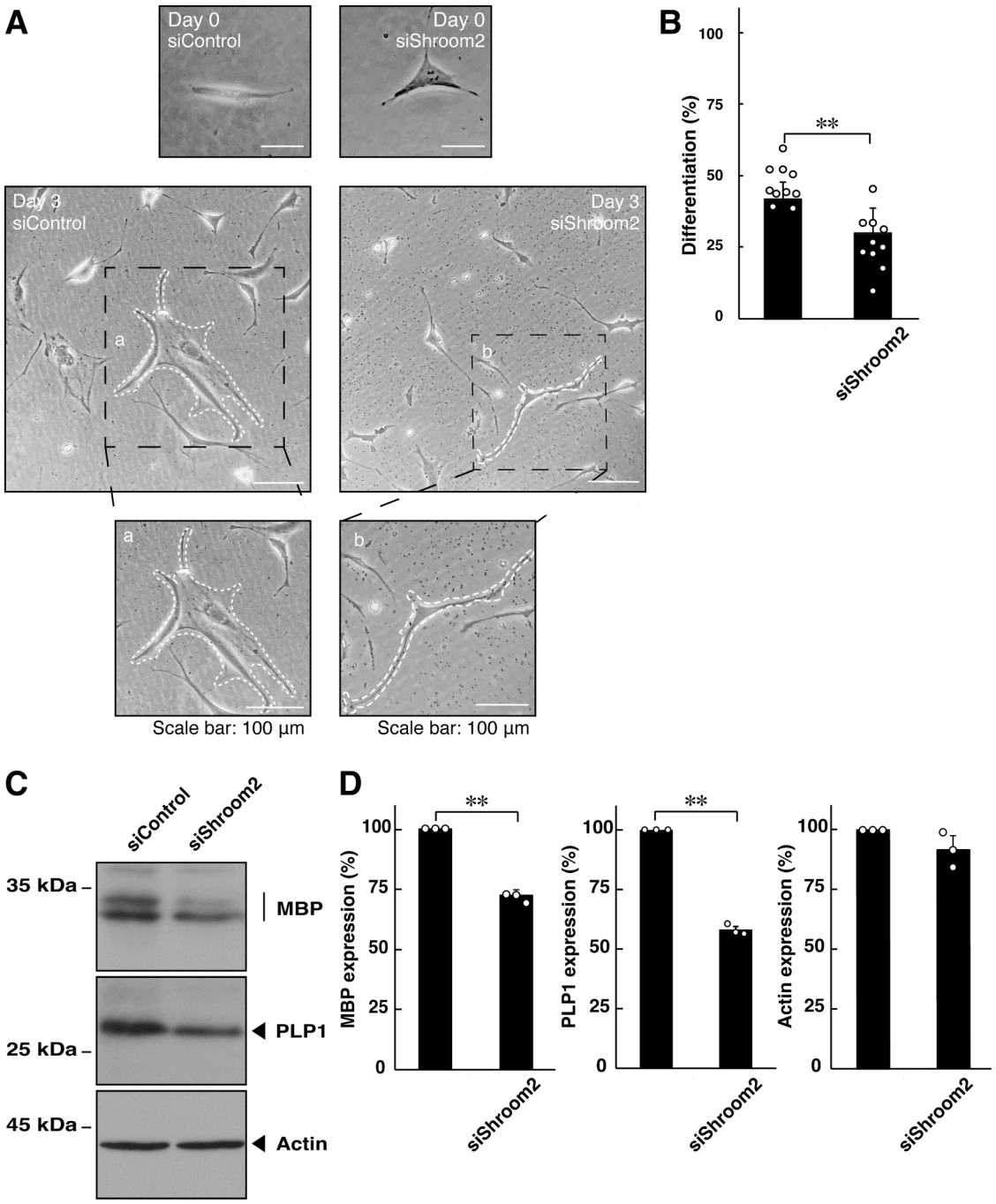

Fig. 4. Knockdown of shroom-2 decreases cell morphology and marker protein expression. (A, B) Cells were transfected with control luciferase siRNA (siControl) or shroom-2 siRNA (siShroom2) and cultured for 0 or 3 days following the induction of differentiation. Cells meeting differentiation criteria were counted and statistically depicted in the graph (** $p < 0.01$; $n = 10$ fields). Panels a and b (lower photographs) are enlarged images of squares a and b surrounded by black dotted lines (middle photographs). Some cells are surrounded by white dotted lines. (C and D) And, cell lysates following the induction of differentiation were immunoblotted with the respective antibodies against differentiation marker proteins MBP and PLP1, as well as the internal control actin. The immunoreactive bands of interest were quantified and graphed, with other immunoreactive bands set to 100 % (** $p < 0.01$; $n = 3$ blots).

co-immunoprecipitation (Figure S6). The Kd value is 3.36 ± 0.18 micromolar, indicating probable direct binding.

Next, we investigated whether the isolated PDZ domain of shroom-2 affects morphological changes. We transfected FBD-102b cells with a plasmid encoding the PDZ domain. The result demonstrated that its transfection led to decreased morphological changes (Fig. 2, A and B). These results were consistent with decreased expression levels of MBP and PLP1 in cells transfected with the PDZ domain (Fig. 2, C and D). Similar results in cell morphogenesis were obtained when the carboxy terminal region of claudin-11 was transfected (Fig. 3, A and B). Also, transfection with the carboxy terminal region of claudin-11 resulted in decreased expression levels of MBP and PLP1 (Fig. 3, C and D).

These results suggest that the interaction between claudin-11 and shroom-2 plays an important role in oligodendroglial cell differentiation.

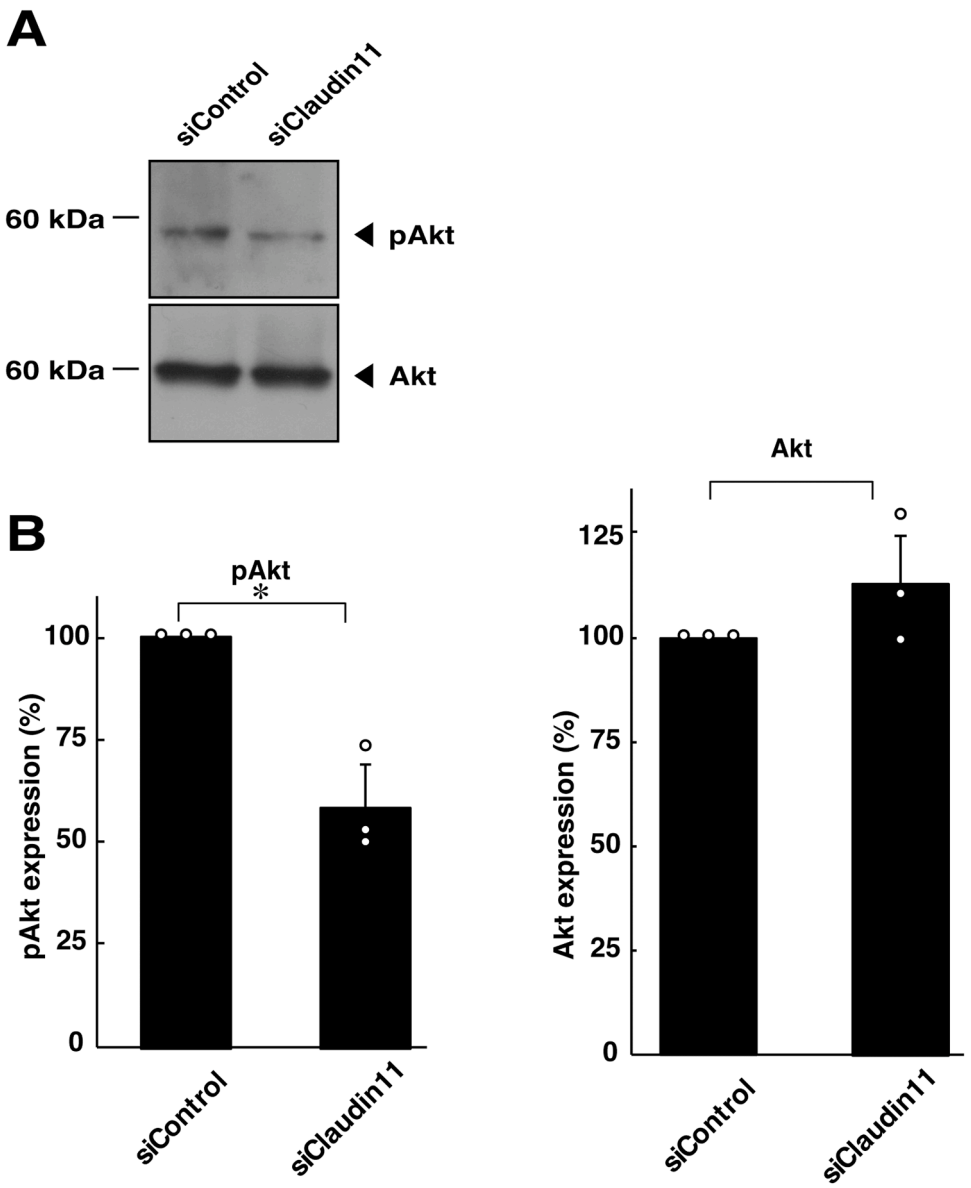

Fig. 5. Knockdown of claudin-11 decreases the phosphorylation level of Akt kinase. (A, B) Cells were transfected with control luciferase siRNA (siControl) or claudin-11 siRNA (siClaudin11) and allowed to differentiate for 2 days. Cell lysates were immunoblotted with the respective antibodies against phosphorylated Akt kinase (pAkt) and total Akt kinase (Akt). The immunoreactive bands of interest were quantified and graphed, with other immunoreactive bands set to 100 % (** $p < 0.01$; $n = 3$ blots).

3.3. Knockdown of shroom-2 decreases morphological changes with decreased differentiation marker proteins

We explored whether shroom-2 itself is involved in the regulation of oligodendroglial cell morphological differentiation by transfecting cells with siRNA specific for shroom-2. Knockdown of shroom-2 (Figure S7) resulted in decreased morphological changes (Fig. 4, A and B) and decreased expression levels of MBP and PLP1 (Fig. 4, C and D) as well as of CNPase and GSTpi (Figure S4, C and D), indicating the key role of shroom-2 in differentiation.

3.4. Knockdown of claudin-11 or shroom-2 leads to decreased Akt kinase phosphorylation

Finally, we examined whether claudin-11 or shroom-2 affects the phosphorylation of Akt kinase, which is essential for oligodendroglial cell differentiation and myelination [26–28]. Knockdown of claudin-11 resulted in decreased phosphorylation of Akt kinase, whereas the expression levels of Akt kinase remained comparable (Fig. 5, A and B; Figure S4, A and B). Similarly, knockdown of shroom-2 also led to decreased phosphorylation of Akt kinase (Fig. 6, A and B; Figure S4, C and D), suggesting that both claudin-11 and shroom-2 positively regulate differentiation.

4. Discussion

Patients with HLDs, including PMD, typically present with head shaking or eye shaking. Parkinsonism symptoms, such as tremor, rigidity, and slowness of movement, are often observed in HLD patients. Leg spasticity, followed by arm spasticity, cerebellar ataxia, and dementia, are common features that appear during the first one or two decades of life. It is believed that many of these severe symptoms result from impaired electrical conduction efficiency through axons due to oligodendroglial cell hypomyelination and/or demyelination. Additionally, since myelin sheaths protect axons, abnormal myelination can result in causing axonal retraction or breakdown. Hypomyelination

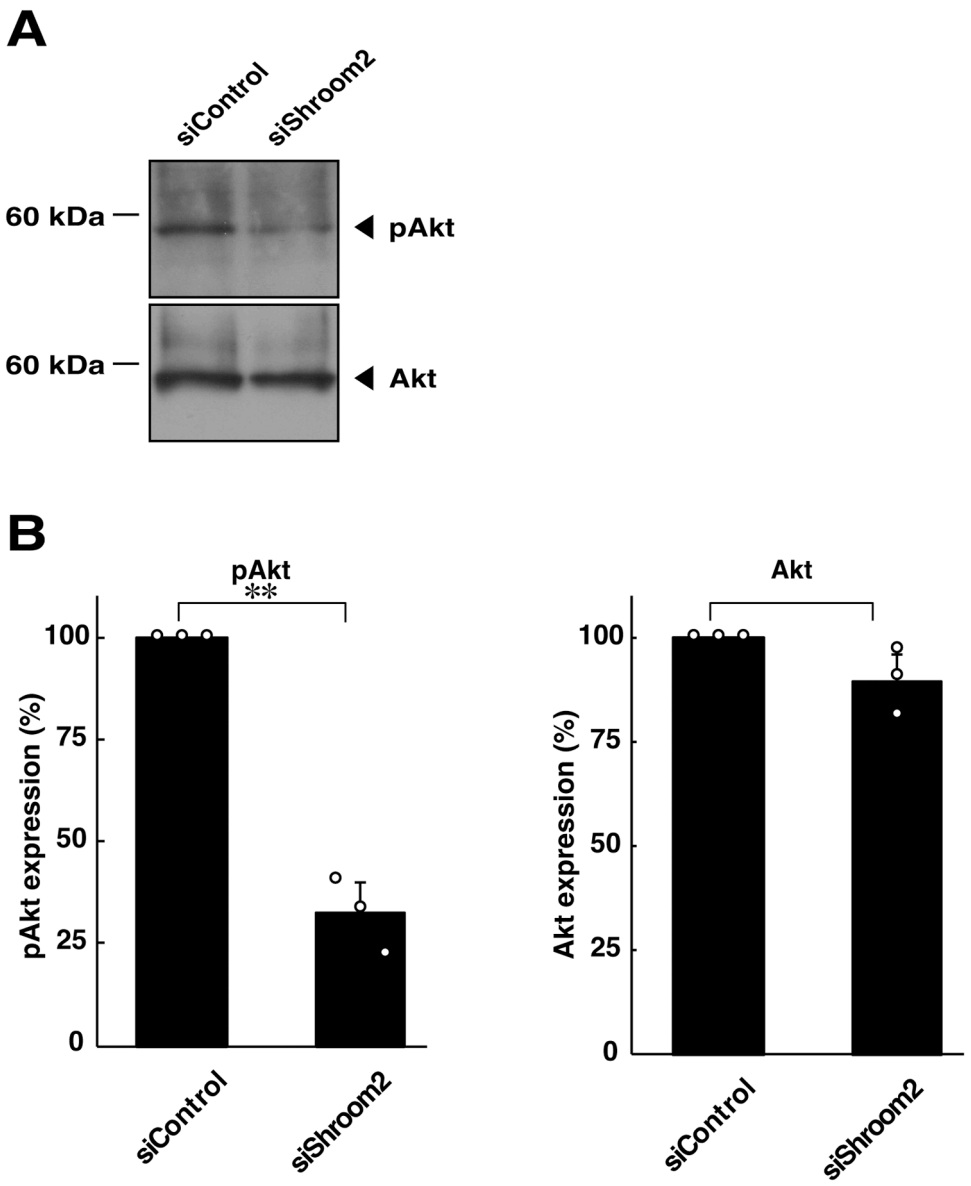

Fig. 6. Knockdown of shroom-2 decreases the phosphorylation level of Akt kinase. (A, B) Cells were transfected with control luciferase siRNA (siControl) or shroom-2 siRNA (siShroom2) and allowed to differentiate for 2 days. Cell lysates were immunoblotted with the respective antibodies against phosphorylated Akt kinase (pAkt) and total Akt kinase (Akt). The immunoreactive bands of interest were quantified and graphed, with other immunoreactive bands set to 100 % (** $p < 0.01$; $n = 3$ blots).

and/or demyelination are thought to result from delayed or defective differentiation of oligodendroglial cells. Therefore, understanding why and how each responsible gene mutation in HLDs leads to impaired oligodendroglial cell differentiation could provide insights for potential molecular and cellular therapeutic procedures.

HLD22 is associated with a carboxyl terminal amino acid sequence elongation generated by a stop codon mutation in the *claudin-11* gene [15], whose gene product is involved in compact myelin formation [16, 17]. Although this elongated sequence on the cytoplasmic side is unlikely to resemble any known peptide sequences in humans, it is predicted to form a typical alpha-helical structure [15]. Since isolated helical structures typically interact with other proteins, this elongated sequence may cause different protein localization through binding to its helical structure. Alternatively, the added sequence could inhibit the formation of normal protein complexes involving claudin-11 on the cytoplasmic side of the plasma membrane. In either case, the additional sequence may disrupt adhesion signaling in both directions, possibly leading to the loss-of-function of claudin-11. In this study, we find that knockdown of claudin-11 decreases morphological changes and reduces the expression levels of oligodendroglial cell differentiation marker proteins. The HLD22-associated mutant claudin-11 (claudin-11 protein with 39 additional amino acids at the carboxyl terminal) fails to interact with the PDZ domain of shroom-2, a newly identified partner of claudin-11. On the other hand, claudin family proteins interact homophilically or heterophilically to form tight junctional complexes [29,30]. It remains unclear whether claudin-11 is involved in tight junction formation between myelin sheaths or between myelin sheaths and axons. However, the deficiency of claudin-11 and its partner shroom-2 interactive ability may affect oligodendroglial cell differentiation and subsequent myelination.

The findings that knockdown of either claudin-11 or shroom-2 decreases morphological changes, and that the carboxyl terminal PDZ of claudin-11 interacts with the PDZ domain of shroom-2, suggest the key role of a claudin-11 and shroom-2 complex in morphological changes. However, overexpression of either the carboxyl terminal PDZ of claudin-11 or the PDZ domain of shroom-2 in cells leads to decreased

morphological changes, even though claudin-11 or shroom-2 can positively contribute to their processes. This is likely because the carboxyl terminal sequence of claudin-11 and the PDZ domain of shroom-2 interact with shroom-2 and claudin-11, respectively, inhibiting the formation of a claudin-11 and shroom-2 complex in cells. In other words, the carboxyl terminal sequence of claudin-11 and the PDZ domain of shroom-2 may act as dominant-negative mutants in cells. Alternatively, these regions could inhibit potential interactions with other partner molecule(s), although it is clear that the interaction between claudin-11 and shroom-2 plays a crucial role in morphological changes.

It has been proposed that shroom-2 not only binds to filamentous actin but also functions as a scaffold protein, acting as an adaptor for cytoskeletal proteins through Rho-kinases (also called Rho-associated coiled-coil containing protein kinase 1/2 [Rock1/2]) inside the plasma membrane [31]. Shroom-2 recruits Rho-kinase to cortical actin, where it activates the myosin regulatory light chain. This signaling mechanism establishes cellular contractility, contributing to the initiation of cell morphological changes in epithelial cell lines [32]. However, it remains unclear what molecules, including claudin family proteins, bind to the PDZ domain. If this protein complex is preserved in oligodendroglial cells, claudin-11 may interact with the PDZ domain to regulate actin cytoskeletal changes. In the tight junction structure, shroom-2 also binds to the scaffold protein ZO-1 to re-arrange actin networks in epithelial cell lines. This interaction between scaffold proteins could expand the variety of cell-cell adhesion signaling. Importantly, specific signaling through cell adhesion complexes in epithelial cells has the potential to promote epithelial differentiation [33], which may be analogous to the molecular events involved in oligodendroglial morphological differentiation. Mutations in shroom-2 among the shroom family proteins are likely associated with neurodevelopmental disorder [34]. Scaffold proteins and their associated complexes inside the plasma membrane may differ depending on cell types; however, claudin-11 may also act upstream of shroom-2 in CNS developmental signaling, including myelination, following oligodendroglial cell morphological differentiation.

The genes responsible for HLD1, HLD2, and HLD22 all encode tetraspan membrane proteins [35–38]. Disease-associated missense mutations and/or amplification of genes encoding HLD1, HLD2, and HLD22 lead to abnormal protein folding of their translational products, resulting in organelle stress in oligodendroglial cells [35,36]. It is likely that this stress signaling leads to insufficient differentiation of oligodendroglial cells and, consequently, hypomyelination [11,12]. Further genomic analyses in HLD22 patients could help clarify the relationship between disease-associated mutations and organelle stress. In fact, the ClinVar website (https://www.ncbi.nlm.nih.gov/clinvar/) identifies several cases of *claudin-11* gene amplification, suggesting that HLD22 may also share the same cause as HLD1. Detailed studies to date have shown that HLD22 is caused by a functional loss due to a point mutation in the stop codon of claudin-11.

In the present study, we demonstrate that knockdown of claudin-11, an HLD22-associated protein, leads to a decrease in the expression levels of oligodendroglial cell differentiation markers and reduced cell morphological changes. Claudin-11 interacts with the PDZ domain of shroom-2, and knockdown of shroom-2 also results in decreased morphological changes. Expression of the respective interactive regions in cells similarly leads to reduced morphological changes, illustrating the key role of the claudin-11 and shroom-2 interaction in cell morphological changes. Of interest, HLD22-associated claudin-11 sequence fails to interact with the PDZ domain of shromm-2. Further studies could promote our understanding of the detailed molecular mechanisms by which claudin-11 promotes differentiation before the onset of myelination in primary and induced oligodendroglial cells [39,40] and in mice, as well as how shroom-2 intracellularly connects the signal from claudin-11. These studies could help identify potential drug targets to effectively promote oligodendroglial myelination and, in turn, lead to the development of therapeutic medicines for HLD22 and related diseases.

CRediT authorship contribution statement

Sakurako Kobayashi: Writing – review & editing, Writing – original draft, Visualization, Validation, Software, Resources, Methodology, Investigation, Formal analysis, Data curation. **Takanori Yokoi:** Visualization, Validation, Software, Resources, Methodology, Investigation, Formal analysis, Data curation. **Takeru Omata:** Methodology, Investigation. **Hideji Yako:** Visualization, Validation, Formal analysis, Data curation. **Yuki Miyamoto:** Writing – review & editing, Writing – original draft, Visualization, Validation, Formal analysis, Data curation. **Junji Yamauchi:** Writing – review & editing, Writing – original draft, Supervision, Project administration, Funding acquisition, Formal analysis, Data curation, Conceptualization.

Declaration of competing interest

The authors declare that they have no known competing financial interests or personal relationships that could have appeared to influence the work reported in this paper.

Acknowledgements

We thank Drs. Takako Morimoto and Yoichi Seki (Tokyo University of Pharmacy and Life Sciences) for their insightful comments throughout this study.

Funding sources

This work was supported by the Core Research for Evolutional Science and Technol3333ogy (CREST) program of the Japan Science and Technology Agency (JST). Additional support was provided by Grants-in-Aid for Scientific Research from the Japanese Ministry of Education, Culture, Sports, Science and Technology (MEXT) and Grants-in-Aid for Medical Scientific Research from the Japanese Ministry of Health, Labour and Welfare (MHLW). We also received funding from the Daiichi Sankyo Science Foundation, Japan Foundation for Pediatric Research, Mishima Kaiun Memorial Foundation, Mitsubishi Tanabe Science Foundation, Otsuka Science Foundation, and Takeda Science Foundation.

Supplementary materials

Supplementary material associated with this article can be found, in the online version, at doi:10.1016/j.bbadva.2025.100159.

Data availability

The datasets used and/or analyzed for the current study are available from the corresponding author upon reasonable request.

References

[1] N. Baumann, D. Pham-Dinh, Biology of oligodendrocyte and myelin in the mammalian central nervous system, Physiol. Rev. 81 (2) (2001) 871–927.
[2] M. Simons, D.A. Lyons, Axonal selection and myelin sheath generation in the central nervous system, Curr. Opin. Cell Biol. 25 (4) (2013) 512–519.
[3] A.S. Saab, K.A. Nave, Myelin dynamics: protecting and shaping neuronal functions, Curr. Opin. Neurobiol. 47 (2017) 104–112.
[4] M. Abu-Rub, R.H. Miller, Emerging cellular and molecular strategies for enhancing central nervous system (CNS) remyelination, Brain Sci 8 (6) (2018) E111.
[5] A. Margiotta, Role of SNAREs and Rabs in myelin regulation, Int. J. Mol. Sci. 24 (2023) 9772.
[6] T. Torii, Y. Miyamoto, J. Yamauchi, Myelination by signaling through Arf guanine nucleotide exchange factor, J. Neurochem. 168 (2024) 2201–2213.
[7] R. Dobson, G. Giovannoni, Multiple sclerosis - a review, Eur. J. Neurol. 26 (2019) 27–40.

[8] M. Haki, H.A. Al-Biati, Z.S. Al-Tameemi, I.S. Ali, H.A. Al-Hussaniy, Review of multiple sclerosis: epidemiology, etiology, pathophysiology, and treatment, Medicine (Baltimore) 103 (2024) e37297.
[9] J. Garbern, F. Cambi, M. Shy, J. Kamholz, The molecular pathogenesis of Pelizaeus-Merzbacher disease, Arch. Neurol. 56 (1999) 1210–1214.
[10] P.J.W. Pouwels, A. Vanderver, G. Bernard, N.I. Wolf, S.F. Dreha-Kulczewksi, S.C. L. Deoni, E. Bertini, A. Kohlschütter, W. Richardson, C. Ffrench-Constant, W. Köhler, D. Rowitch, A., .J.. Barkovich, Hypomyelinating leukodystrophies: translational research progress and prospects, Ann. Neurol. 76 (1) (2014) 5–19.
[11] N.I. Wolf, C. Ffrench-Constant, M.S. van der Knaap, Hypomyelinating leukodystrophies-unravelling myelin biology, Nat. Rev. Neurol. 17 (2021) 88–103.
[12] T. Torii, J. Yamauchi, Molecular pathogenic mechanisms of hypomyelinating leukodystrophies (HLDs), Neurol. Int. 15 (3) (2023) 1155–1173.
[13] A.S. Dhaunchak, D.R. Colman, K.A. Nave, Misalignment of PLP/DM20 transmembrane domains determines protein misfolding in Pelizaeus-Merzbacher disease, J. Neurosci. 31 (42) (2011) 14961–14971.
[14] K. Inoue, Pelizaeus-Merzbacher disease: molecular and cellular pathologies and associated phenotypes, Adv. Exp. Med. Biol. (2019 1190) 201–216.
[15] K.M. Riedhammer, S. Stockler, R. Ploski, M. Wenzel, B. Adis-Dutschmann, U. Ahting, B. Alhaddad, A. Blaschek, T.B. Haack, R. Kopajtich, J. Lee, V. Murcia Pienkowski, A. Pollak, K. Szymanska, M. Tarailo-Graovac, R. van der Lee, C.D. van Karnebeek, T. Meitinger, I. Krägeloh-Mann, K. Vill, De novo stop-loss variants in CLDN11 cause hypomyelinating leukodystrophy, Brain 144 (2021) 411–419.
[16] E.J. Arroyo, S.S. Scherer, On the molecular architecture of myelinated fibers, Histochem. Cell Biol. 113 (2000) 1–18.
[17] S.C. Gjervan, O.K. Ozgoren, A. Gow, S. Stockler-Ipsiroglu, M.A. Pouladi, Claudin-11 in health and disease: implications for myelin disorders, hearing, and fertility, Front. Cell Neurosci. 17 (2024) 1344090.
[18] K.J. Maheras, M. Peppi, F. Ghoddoussi, M.P. Galloway, S.A. Perrine, A. Gow, Absence of claudin 11 in CNS myelin perturbs behavior and neurotransmitter levels in mice, Sci. Rep. 8 (2018) 3798.
[19] M. Horiuchi, Y. Tomooka, An oligodendroglial progenitor cell line FBD-102b possibly secretes a radial glia-inducing factor, Neurosci. Res. 56 (2006) 213–219.
[20] A. Okada, Y. Tomooka, A role of Sema6A expressed in oligodendrocyte precursor cells, Neurosci. Lett. 539 (2013) 48–53.
[21] Y. Miyamoto, T. Torii, M. Terao, S. Takada, A. Tanoue, H. Katoh, J. Yamauchi, Rnd2 differentially regulates oligodendrocyte myelination at different developmental periods, Mol. Biol. Cell 32 (2021) 769–787.
[22] N. Fukushima, Y. Miyamoto, J. Yamauchi, CRISPR/CasRx-mediated knockdown of Rab7B restores incomplete cell shape induced by Pelizaeus-Merzbacher disease-associated PLP1 p.Ala243Val, Neurosci. Insights 19 (2024) 26331055241276873.
[23] C. Achilla, T. Papavramidis, L. Angelis, A. Chatzikyriakidou, The implication of X-linked genetic polymorphisms in susceptibility and sexual dimorphism of cancer, Anticancer Res 42 (2022) 2261–2276.
[24] W. Liu, L. Xiu, M. Zhou, T. Li, N. Jiang, Y. Wan, C. Qiu, J. Li, W. Hu, W. Zhang, J. Wu, The critical role of the shroom family proteins in morphogenesis, organogenesis and disease, Phenomics 4 (2024) 187–202.
[25] A. Ochiai, S. Sawaguchi, S. Memezawa, Y. Seki, T. Morimoto, H. Oizumi, K. Ohbuchi, M. Yamamoto, K. Mizoguchi, Y. Miyamoto, J. Yamauchi, Knockdown of Golgi stress-responsive caspase-2 ameliorates HLD17-associated AIMP2 mutant-mediated inhibition of oligodendroglial cell morphological differentiation, Neurochem. Res. 47 (2022) 2617–2631.
[26] G. Figlia, D. Gerber, U. Suter, Myelination and mTOR, Glia 66 (2018) 693–707.
[27] Q. Yu, T. Guan, Y. Guo, J. Kong, The initial myelination in the central nervous system, ASN Neuro 15 (2023) 17590914231163039.
[28] K.D. Dahl, A.R. Almeida, H.A. Hathaway, J. Bourne, T.L. Brown, L.T. Finseth, T. L. Wood, W.B. Macklin, mTORC2 loss in oligodendrocyte progenitor cells results in regional hypomyelination in the central nervous system, J. Neurosci. 43 (2023) 540–558.
[29] S. Tsukita, H. Tanaka, A. Tamura, The claudins: from tight junctions to biological system, Trends Biochem. Sci. 44 (2019) 141–152.
[30] S. Citi, M. Fromm, M. Furuse, L. González-Mariscal, A. Nusrat, S. Tsukita, J. R. Turner, A short guide to the tight junction, J. Cell Sci. 137 (2024) jcs261776.
[31] M.J. Farber, R. Rizaldy, J.D. Hildebrand, Shroom2 regulates contractility to control endothelial morphogenesis, Mol. Biol. Cell 22 (2011) 795–805.
[32] R. Etournay, I. Zwaenepoel, I. Perfettini, P. Legrain, C. Petit, A. El-Amraoui, Shroom2, a myosin-VIIa- and actin-binding protein, directly interacts with ZO-1 at tight junctions, J. Cell Sci. 120 (2007) 2838–2850.
[33] B. Boëda, V. Michel, R. Etournay, P. England, S. Rigaud, H. Mary, S. Gobaa, S. Etienne-Manneville, SCRIB controls apical contractility during epithelial differentiation, J. Cell Biol. 222 (2023) e202211113.
[34] Z. Chen, L. Kuang, R.H. Finnell, H. Wang, Genetic and functional analysis of SHROOM1-4 in a Chinese neural tube defect cohort, Hum. Genet. 137 (2018) 195–202.
[35] M.S. Elitt, P.J. Tesar, Pelizaeus-Merzbacher disease: on the cusp of myelin medicine, Trends Mol. Med. 30 (2024) 459–470.
[36] S. Perrier, L. Gauquelin, G. Bernard, Inherited white matter disorders: hypomyelination (myelin disorders), Handb. Clin. Neurol. 204 (2024) 197–223.
[37] C.K. Abrams, Mechanisms of diseases associated with mutation in GJC2/connexin 47, Biomolecules 13 (2023) 712.
[38] A. Ghasemi, A.R. Tavasoli, M. Khojasteh, M. Rohani, A. Alavi, Description of phenotypic heterogeneity in a GJC2-related family and literature review, Mol. Syndromol. 14 (2023) 405–415.
[39] M.K. Schreiber, M.P. Zafeiriou, Generation of Pelizaeus-Merzbacher disease (PMD) mutant (PLP1-C33Y) in induced pluripotent stem cell (iPSC) by CRISPR/Cas9 genome editing, Stem Cell Res 74 (2024) 103276.
[40] M.K. Schreiber, M.P. Zafeiriou, Generation of a fluorescent oligodendrocyte reporter line in human induced pluripotent stem cells, Stem Cell Res 75 (2024) 103295.